Weak itinerant ferromagnetism in Heusler-type Fe2VAl0.95

Sato, K.; Naka, T.; Taguchi, M.; Nakane, T.; Ishikawa, F.; Yamada, Y.; Takaesu, Y.; Nakama, T.; de Visser, A.; Matsushita, A.

DOI
10.1103/PhysRevB.82.104408

Publication date
2010

Document Version
Final published version

Published in
Physical Review B

Weak itinerant ferromagnetism in Heusler-type $Fe_2VAl_{0.95}$

K. Sato,[1] T. Naka,[1,*] M. Taguchi,[1] T. Nakane,[1] F. Ishikawa,[2] Y. Yamada,[3] Y. Takaesu,[4] T. Nakama,[4] A. de Visser,[5] and A. Matsushita[1]

[1]*National Institute of Materials Science, Tsukuba, Sengen 1-2-1, Tsukuba, Ibaraki 305-0047, Japan*

[2]*Graduate School of Science and Technology, Niigata University, 8050, Igarashi Niigata 950-2181, Japan*

[3]*Department of Physics, Faculty of Science, Niigata University, 8050, Igarashi Niigata 950-2181, Japan*

[4]*Faculty of Science, University of the Ryukyus, Nishihara, Okinawa 903-0213, Japan*

[5]*Van der Waals-Zeeman Institute, University of Amsterdam, Valckenierstraat 65, Amsterdam 1018 XE, The Netherlands*

(Received 11 May 2010; revised manuscript received 12 July 2010; published 8 September 2010)

We report measurements of the magnetic, transport, and thermal properties of the Heusler-type compound $Fe_2VAl_{0.95}$. We show that while stoichiometric Fe_2VAl is a nonmagnetic semimetal a 5% substitution on the Al site with the 3*d* elements Fe and V atoms leads to a ferromagnetic ground state with a Curie temperature $T_C=33\pm3$ K and a small ordered moment $\mu_s=0.12\mu_B$/Fe in $Fe_2VAl_{0.95}$. The reduced value of the ratio $\mu_s/\mu_p=0.08$, where $\mu_p=1.4\mu_B$/Fe is the effective Curie-Weiss moment, together with the analysis of the magnetization data $M(H,T)$, show magnetism is of itinerant nature. The specific heat shows an unusual temperature variation at low temperatures with an enhanced Sommerfeld coefficient, $\gamma=12$ mJ K^{-2} mol^{-1}. The resistivity, $\rho(T)$, is metallic and follows a power law behavior $\rho=\rho_0+AT^n$ with $n\approx1.5$ below T_C. With applying pressure, T_C decreases with the rate of $(1/T_C)(dT_C/dP)=-0.061$ GPa^{-1}. We conclude substitution on the Al site with Fe and V atoms results in itinerant ferromagnetism with a low carrier density.

DOI: 10.1103/PhysRevB.82.104408 PACS number(s): 75.30.Kz, 71.20.Be, 75.47.−m

I. INTRODUCTION

Weak ferromagnetic (or antiferromagnetic) transition metal and rare earth or actinide metallic compounds are intensively investigated, since novel ground states, such as heavy fermion behavior, non-Fermi-liquid states and unconventional superconductivity, may emerge at low temperatures. These exotic phases are located at the boundary of magnetically ordered states, and may be reached by tuning the ground state by chemical pressure (alloying), mechanical pressure and/or applying an external magnetic field. Heusler- and semi-Heusler-type of compounds composed of transition metals form an attractive materials family to investigate novel emerging phenomena, the more because these are candidates for half metallic states, in which the band electrons are fully spin polarized.[1,2] In the magnetically ordered state of half metals, the exchange gap is quite large and the minority spin band is fully occupied. This might be of practical use in spin sensitive devices,[3] which provides a second reason why Heusler-type compounds are investigated intensively. Since applications demand both a high spin polarization and stable ferromagnetism above room temperature, this is an exigent and challenging mission.

Although the concept of the half-metal comes truly from an itinerant electron picture, one can address the question how much local moment character strongly spin-polarized metals possess.[4,5] In fact, it is well known that in nearly and weak ferromagnetic itinerant electron systems, such as $ZrZn_2$ and MnSi, the conduction electrons are responsible for both the itinerant and localized electron nature (i.e., the Curie-Weiss behavior in magnetic susceptibility). For a few candidate materials only the low-temperature magnetic and thermal properties could be analyzed satisfactorily in the framework of itinerant electron magnetism. We mention the semi-Heusler-type ferromagnet NiMnSb (Ref. 4) and antiferromagnet CuMnSb,[5] which were examined under magnetic field and high pressure.

In this paper we focus on the magnetic transition and the low-temperature properties of the Heusler-type iron-vanadium compound, $Fe_2VAl_{0.95}$. Fe_2VAl and related alloys have attracted considerable attention[6–11] since it was claimed that these 3*d*-electron systems with small carrier concentration, $n\approx0.01$ per unit formula,[7] exhibit a significant carrier mass enhancement and non-Fermi-liquid behavior.[6] Stoichiometric Fe_2VAl is nonmagnetic and related alloys, such as $Fe_{2+x}V_{1-x}Al$ and $Fe_2VAl_{1-\delta}$, exhibit ferromagnetic transitions.[7,10–14] Consequently, the samples at $x\approx0$ and $\delta\approx0$ are located at the brink of ferromagnetic order, close to the ferromagnetic quantum critical point, i.e., $T_C\rightarrow0$.[6,8] Stimulated by these findings, theoretical work claimed Fe_2VAl is a nonmagnetic semimetal with the pseudogap at the Fermi level.[15–17] The considerable mass enhancement of the conduction carriers was attributed to excitonic correlations[16] or spin fluctuations.[17] However, subsequent specific heat, $C(T)$, measurements in applied magnetic fields showed that the upturn in C/T at low temperatures results from a Schottky contribution of magnetic clusters in Fe_2VAl.[8] The effects of off-stoichiometry have not been investigated quantitatively in the framework of nearly and weak ferromagnetism at $x\approx0$ and $\delta\approx0$ yet. Another interesting aspect of Fe_2VAl is its potential for application in thermoelectric devices, since off-stoichiometry and heat-treatment procedures may results in an enhancement of the Seebeck coefficient.[6,11,12] In $Fe_{2+x}V_{1-x}Al$ (Refs. 11 and 12) and $Fe_2VAl_{1-\delta}$,[12] the thermoelectric power is enhanced for $x\approx0$ and $\delta\approx0$: with a negative sign for $x<0$ and $\delta>0$, and positive sign for $x>0$ and $\delta<0$. In the case of stoichiometric Fe_2VAl the negative temperature coefficient in the electrical resistivity observed up to 1300 K and the constant value of the Hall coefficient at low temperatures[6,7,12] suggest it is a low carrier-density semimetal with a pseudogap at the

Fermi level.[6] Antisite defects and magnetic nanoclusters induced by heat treatment and nominal off-stoichiometry bring about ferromagnetism[7,10,13,18] and superparamagnetism.[18] With increasing x in $Fe_{2+x}V_{1-x}Al$, the excess of Fe atoms occupy the nominal V site and, consequently, Fe_3Al (Fe_2FeAl) clusters are formed [notice bulk Fe_3Al is ferromagnetic with $T_C=803$ K (Refs. 6 and 13)]. The presence of antisite Fe atoms on the nominal V site in the FeV_2Al system brings about a simultaneous enhancement of the magnetization and resistivity at low temperatures.[7,9,10] This led to the claim that localized magnetic moments must be a crucial factor in the strong magnetic scattering of the conduction electrons responsible for the steep rise of the resistivity, the negative temperature coefficient of the resistivity, $d\rho/dT<0$ and a giant magnetoresistance at $x>0$. Thus it is proposed that the steep rise of the electrical resistivity at lower temperature is not due to the energy gap but due to strong magnetic scattering.[7,9,10]

Al poor $Fe_2VAl_{1-\delta}$ ($\delta>0$), seems to undergo a ferromagnetic transition and shows metallic conduction below room temperature.[12] The $Fe_2VAl_{1-\delta}$ system at $\delta>0$ yields the opportunity to examine quantitatively not only the magnetic but also the transport and thermal properties within the framework of itinerant electron ferromagnetism, as established for intermetallic compounds, such MnSi and $ZrZn_2$.[19] In this paper we report a comprehensive study of the low temperature bulk properties of $Fe_2VAl_{0.95}$, notably magnetization, electrical resistivity, and specific-heat measurements. Whereas, as pointed out above, the magnetism in $Fe_{2+x}V_{1-x}Al$ is considered to be due to magnetic clusters having a semilocalized nature,[8] our results on $Fe_2VAl_{0.95}$ show it is a weak ferromagnet, with a bulk magnetic transition at $T_C=33$ K and a low carrier concentration $n\approx0.06$.

II. EXPERIMENTAL

Polycrystalline samples of $Fe_2VAl_{0.95}$, Fe_2VAl, and $Fe_2VAl_{1.05}$ were prepared by arc melting the proper amounts of elements into the nominal chemical composition. The samples were subjected to a heat treatment at 1000 °C for 15 h for homogenization purposes, and next annealed at 400 °C for 15 h. For all samples the crystal structure was identified as the Heusler-type. No secondary phases were detected in the powder x-ray diffraction (XRD) profiles. Since after annealing the grain size (i.e., the individual crystallite size) in the polycrystalline samples is quite large (>several hundredths μm), we expect that the volume fraction of impurity phases located at the grain boundaries is quite low. The samples we report on in this work are the same as those previously characterized by XRD, scanning electron microscope (SEM), and energy dispersive x-ray spectroscopy (EDS).[7]

dc-magnetization, four-probe ac electrical resistivity and specific-heat measurements down to $T=2$ K were carried out using a conventional superconducting quantum interference device magnetometer and a physical property measurement system (Quantum Design), respectively. Resistivity measurements down to $T=0.23$ K were carried out in a ^{3}He refrigerator (Heliox VL, Oxford Instruments) with a sensitive

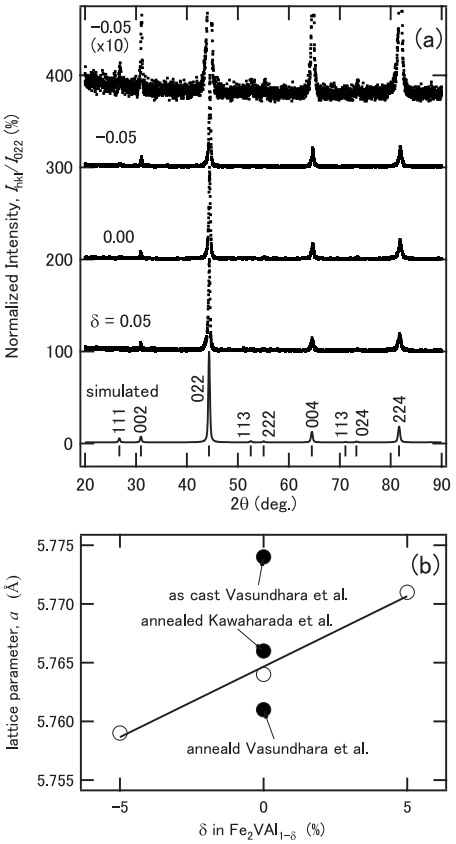

FIG. 1. (a) X-ray diffraction patterns of $Fe_2VAl_{1-\delta}$ at $\delta=-0.05, 0.00, 0.05$ and a simulated one for Fe_2VAl with the Heusler structure. The top XRD pattern of $\delta=-0.05$ is magnified ten times vertically. Ticks and numbers being along the simulated pattern indicate the position of the Bragg reflections and corresponding Miller indices, respectively, for the Heusler structure. (b) Lattice parameters obtained in this work as a function of δ (open circle). Solid line is a guide for eyes. Solid circles at $\delta=0$ represent reported values in Refs. 18 and 20.

LR700 (Linear Research) ac resistance bridge at the Van der Waals-Zeeman Institute of the University of Amsterdam. In the high-pressure measurement, a handmade measurement system specialized for high-pressure measurement with a glass Dewar vessel was used. To generate high pressure a hybrid clamp cell made from nonmagnetic NiCrAl and CuBe alloys was used. The sample was mounted on a specially designed plug and put inside a Teflon cell with the pressure-transmitting medium Daphne 7373 (Idemitsu).

III. RESULTS AND DISCUSSION

A. Crystallographic

X-ray diffraction patterns of $Fe_2VAl_{1-\delta}$ at $\delta=-0.05$, 0, and 0.05 are apparently identified to be of the single phase Heusler-type (Cu_2MnAl) structure in the space group $Fm\bar{3}m$. A as shown in Fig. 1(a), no impurity phases were detected, except for small amounts of Al and Al oxide inclusions indicated by SEM and EDS measurements.[7] Therefore, we expect, the actual Al composition, δ, is slightly smaller than the

nominal one. Figure 1(b) shows the δ dependence of lattice constant, a, estimated in this work with those reported in previous works[18,20] for comparison. The lattice constant at $\delta=0$ measured in this work corresponds well with those for annealed samples. The linear dependence of a versus δ supported that the excess Fe and V atoms occupy the Al site for $\delta>0$ and the excess Al atom locates at the Fe and/or V site(s) for $\delta<0$, since Al has smaller ionic radius than those of Fe and V.

As shown below (see Sec. III C), the resistivity versus temperature curve obtained for $\delta=0.05$ is quite similar to those reported by Nishino *et al.*[12] Rounded maxima in the resistivity were observed at $T_{max}^{low}=40$ K and $T_{max}^{high}=250$ K in a sample with composition $(Fe_{2/3}V_{1/3})_{75.7}Al_{24.3}$,[12] which corresponds to $\delta=0.035$ in the notation $Fe_2VAl_{1-\delta}$ used here. The maximum at $T=40$ K in the resistivity for $\delta=0.035$ locates the Curie temperature slightly lower than $T_{max}^{low}=50$ K of $\delta=0.05$ observed in this work [Fig. 5(a)]. Following the argument of the effect of off-stoichiometry based on the rigid band model[12,21] which is consistent with the Al content variations of the sign in Seebeck and Hall coefficients,[7,12] we are convinced that the excess Fe and V atoms in $Fe_2VAl_{1-\delta}$ occupy the Al site for $\delta>0$, and vice-versa. Actually, it was shown recently by comprehensive magnetic and transport studies in the vicinity of $\delta\approx0$ that not only the Curie point, T_C, but also the saturation moment, μ_s, shows a continuous variation as a function of δ.[22]

B. Magnetization

In Fig. 2(a) we show the magnetization of $Fe_2VAl_{0.95}$ as a function of magnetic field, $M(H)$, measured at various fixed temperatures. A spontaneous moment appears in the temperature range $T=30-40$ K, which indicates ferromagnetic order [see Fig. 4(a)]. In Fig. 2(b) we have traced the temperature variation in the magnetic susceptibility, $\chi(T)$, measured in a field of 20 kOe. As indicated by the straight line in the plot of $1/\chi(T)$ versus T the susceptibility follows a Curie-Weiss law, $\chi(T)=C/(T-\theta)$, for $T>100$ K, from which we extract the Curie constant $C=0.243$ emu K/g and a Curie-Weiss temperature $\theta=51$ K. By using $C=N\mu_p^2\mu_B^2/3k_B$, an effective magnetic moment $\mu_p=1.4\mu_B$/Fe is obtained, where N, μ_B, and k_B are the number of magnetic (Fe) atoms, the Bohr magneton and Boltzmann's constant, respectively. This value of μ_p is considerably larger than that of heat-treated Fe_2VAl ($\mu_p\sim0.2\mu_B$/Fe).[23] The saturation moment at $T=2$ K is $\mu_s=0.12\mu_B$/Fe, which is much smaller than the paramagnetic moment, $\mu_p=1.4\mu_B$/Fe. The small value of the ratio $\mu_s/\mu_p=0.083$ corroborates the itinerant electron nature of ferromagnetism in $Fe_2VAl_{0.95}$. It is noteworthy that an Al-site substitution of only 5% ($\delta=0.05$) modifies the magnetic properties strongly: the appearance of a spontaneous moment and low magnetic transition temperature and a strong enhancement of the paramagnetic moment. We stress that these changes cannot be due to an impurity phase, like for instance $Fe_{1-x}V_x(x=1/3)$, for which the estimated values of μ_p and μ_s are one order of magnitude larger than those observed and T_C is above room temperature.[24] In contrast with the observations concerning magnetism in annealed Fe_2VAl (Ref. 18) and $Fe_2V_{1-x}Cr_xAl$,[25] the ferromagnetic transition in $Fe_2VAl_{0.95}$ is also signaled: (i) in the temperature derivative of the resistivity, $(1/\rho)(d\rho/dT)$, shown in Fig. 5(b), (ii) by the temperature variation of the specific heat divided by temperature, C/T, showing a λ-peaklike shape [Fig. 9(b)], (iii) by the M^4-M/H plot [Fig. 3(a)], and (iv) by the M^2-$(T/T_C)^{4/3}$ plot [Fig. 4(a)]. Notably, the transition temperatures $T_C=33\pm3$ K determined by the different techniques agree within the uncertainty of 3 K. Correspondingly, both coercive force, H_c, and remanent magnetization, M_r, emerge around T_C [Fig. 2(b)].

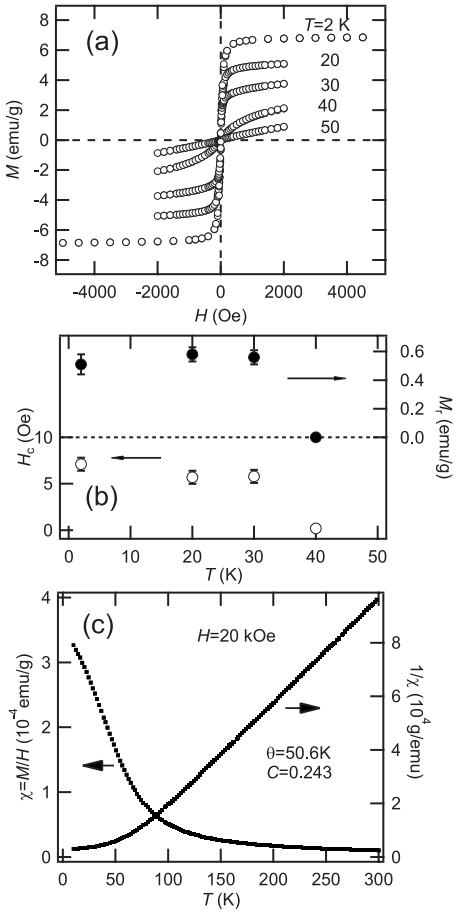

FIG. 2. (a) Magnetization versus field (M-H) of $Fe_2VAl_{0.95}$ at fixed temperatures as indicated. (b) Coersive force, H_c, and remanent magnetization, M_r, as a function of temperature. (c) Magnetic susceptibility, $\chi(T)=M/H$, and reciprocal susceptibility, $1/\chi(T)$, as a function of temperature measured in a fixed field $H=20$ kOe. The susceptibility is expressed in units per gram.

As mentioned in Sec. I, it is interesting to examine whether magnetism in $Fe_2VAl_{0.95}$ has an itinerant or localized character. In the latter case it is expected that the induced spin is localized at the $3d$ atoms (Fe or V) substituted on the Al site. In Figs. 3(a) and 3(b) we analyze the magnetization data around T_C in terms of M^4-H/M and M^2-H/M (Arrott) plots, respectively. For weak ferromagnetic systems the M^4 versus H/M curve at $T=T_C$ is predicted to be linear with an intercept zero.[26] Inspecting Fig. 2(a) we conclude $T_C=33$ K. Notice, in the Arrott plot the M^2 versus H/M curves all exhibit a strong curvature toward the H/M axis.

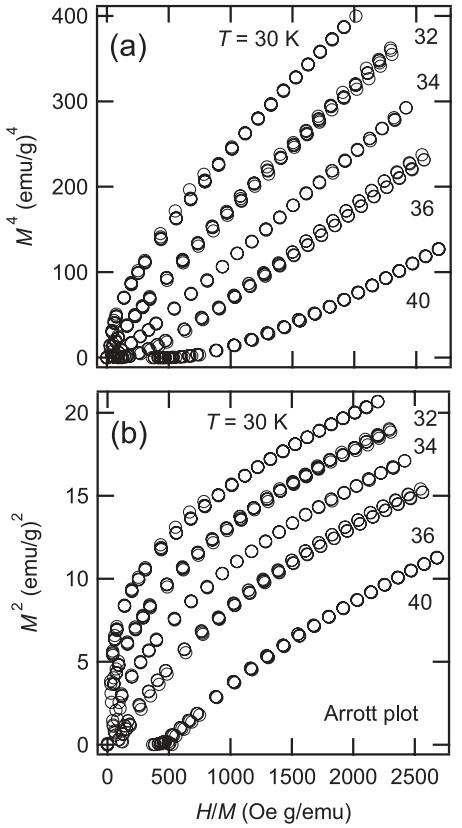

FIG. 3. Magnetization of $Fe_2VAl_{0.95}$ measured at fixed temperatures as indicated, plotted as (a) M^4 versus H/M and (b) M^2 *versus* H/M (Arrott plot).

This feature is quite similar to those found in prototypical itinerant ferromagnets, such as MnSi and Ni_3Al.[26] Thus the magnetization data provide strong evidence for itinerant ferromagnetism with $T_C=33$ K in $Fe_2VAl_{0.95}$. Based on the generalized Rhodes-Wohlfarth plot,[26] we obtain the characteristic temperature $T_0=895$ K for $Fe_2VAl_{0.95}$. The ratio T_C/T_0 is an important parameter as it characterizes the degree of localization or itineracy of the spin moment.[19] For $T_C/T_0 \ll 1$ the magnetic material has a strong itinerant character while at $T_C \sim T_0$ local moment magnetism results. The estimated value $T_C/T_0=0.038$ is comparable to the values reported for MnSi (0.13), Ni_3Al (0.0116), $ZrZn_2$ (0.053), and Sc_3In (0.0097) which all exhibit weak ferromagnetism.[26] With help of T_0, one may calculate the temperature dependence of the magnetization below T_C. With decreasing T_C/T_0 the $M(T)$ curve deviates more and more from the mean-field behavior, $M=M(0)[1-(T/T_C)^2]^{1/2}$, and has a tendency to follow $M=M(0)[1-(T/T_C)^{4/3}]^{1/2}$. In fact, as shown in Fig. 4(b), $M^2(T)$ of $Fe_2VAl_{0.95}$ obeys the $T^{4/3}$ dependence for a weak itinerant ferromagnet rather than the T^2 dependence of the mean-field model.[26] By using $M(T)=M(0)[1-(T/T_C)^{4/3}]^{1/2}$ the zero-temperature magnetization and Curie point are estimated to be $M(0)=5.7$ emu/g and $T_C=36$ K at $H=200$ Oe, respectively.

C. Electrical resistivity

In Fig. 5(a) we show the temperature dependence of the resistivity, $\rho(T)$. The resistivity, $\rho(T)$, exhibits rounded

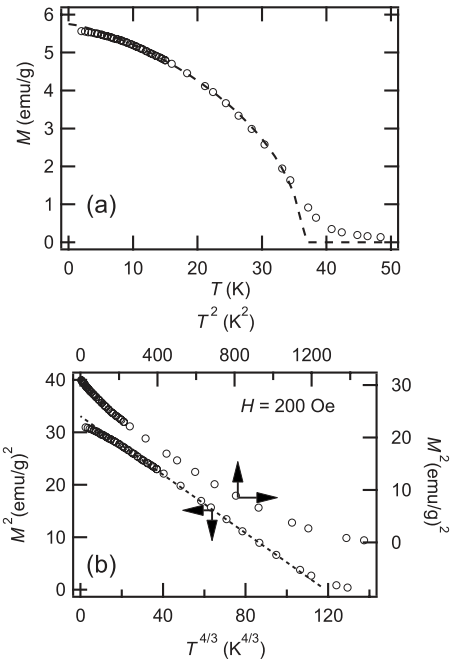

FIG. 4. (a) Magnetization in a field $H=200$ Oe as a function of temperature for $T<50$ K. (b) M^2-$T^{4/3}$ and M^2-T^2 plots measured in a field $H=200$ Oe. The dashed lines are calculated by using $M^2(T)=M(0)[1-(T/T_C)^{4/3}]^{1/2}$ with $M(0)=5.7$ emu/g and $T_C=36$ K obtained by a least-square fit.

maxima at $T_{max}^{low}=52$ K and $T_{max}^{high}=260$ K. A comparison with $Fe_{2+x}V_{1-x}Al$ at $x \approx 0$ (Refs. 7, 10, and 14) reveals that the resistivity above $T \sim 260$ K is dominated by scattering due to thermal excitations in the pseudogap. Below $T \sim 260$ K

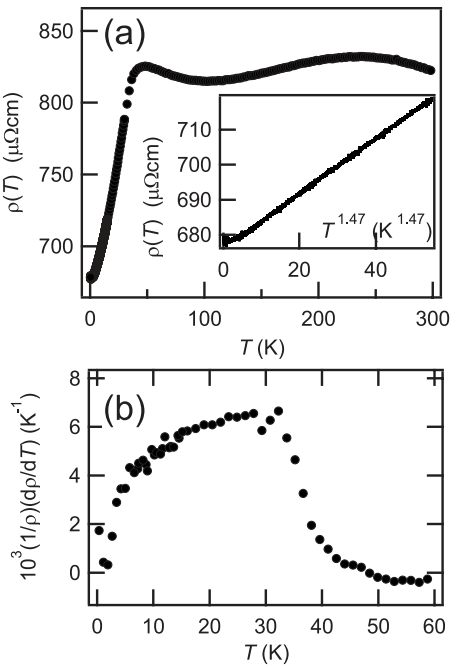

FIG. 5. (a) Resistivity $\rho(T)$ as a function of temperature at $H=0$. Inset: resistivity below T_C plotted as a function of $T^{1.47}$. (b) Temperature variation of $(1/\rho)(d\rho/dT)$. The slope change at $T=33$ K signals T_C.

$\rho(T)$ exhibits metallic behavior, with a low carrier number.[7] On the other hand, the maximum at $T_{max}^{low}=52$ K is caused by the para-to-ferromagnetic phase transition, as was also observed in the Fe-rich composition of $Fe_{2+x}V_{1-x}Al$.[7,10,14] In $Fe_2VAl_{0.95}$ $\rho(T)$ remains metallic down to $T\sim 1$ K, while in the case of $Fe_{2+x}V_{1-x}Al$, especially for $x\leq 0.05$, a semiconductor behavior is reported. The latter was corroborated by weak localization effects of the carriers in a random potential.[9] As shown in Fig. 5(b), the sharp anomaly in $(1/\rho)(d\rho/dT)$ is indicative of a bulk ferromagnetic transition at $T=33$ K. In the ferromagnetic phase the resistivity follows a power law behavior $\rho(T)\sim T^n$ with $n\cong 3/2$ [see inset to Fig. 5(a)]. Notice, it was derived by the self-consistent renormalization (SCR) theory that the temperature dependence of ρ should follow a power law $\sim AT^2$ at $T<T_C$.[19]

D. Magnetoresistance and low-temperature electrical resistivity

The itinerant ferromagnetic character of $Fe_2VAl_{0.95}$ is also reflected in the transverse magnetoresistance (TMR), $[\rho(H)-\rho(0)]/\rho(0)$, especially around $T=T_C$, as shown in Fig. 6(a). The TMR is negative below 100 K and has a minimum at a temperature slightly above T_C. The TMR reaches a maximum size of -11% at $T=43$ K in $H=80$ kOe. The negative temperature coefficient between 50 K$<T<$100 K and the maximum in $\rho(T)$ slightly above T_C are wiped out above $H=30$ kOe, as shown in Fig. 6(a). According to a numerical calculation based on the SCR theory,[27] the negative magnetoresistance is due to the presence of spin fluctuations above T_C and, consequently, the maximum temperature in the TMR shifts toward higher temperature with increasing magnetic field. This field dependence of TMR is comparable with that in the itinerant ferromagnet Sc_3In ($T_C=5.3$ K).[27,28] For $T>100$ K, the TMR is positive. These transport data differ from those in nonmagnetic $Fe_{1.98}V_{1.02}Al$,[7] where $\rho(T)$ exhibits a rounded maximum around room temperature and the magnetoresistance is negative. Remarkably, the temperature dependence of the resistivity changes to $\rho=\rho_0+AT^2$ below a certain temperature T^*, which increases magnetic field [Fig. 6(b)]. This feature is quite similar to that of non-Fermi-liquid systems, such as $U_3Ni_3Sn_4$ where the Fermi-liquid behavior is recovered under magnetic field or external pressure.[29]

E. Pressure effects on resistivity

As mentioned above, crystallographic and chemical defects affect strongly on the magnetic grand state of Fe_2VAl and related alloys.[7] Remarkably, lattice constant of Fe_2VAl reflects sensitively these structural deviations from the Heusler structure.[18] Plausibly, Curie temperature, T_C, is a function of not only carrier number but also the variation of lattice constant, $\Delta a/a$. To distinguish those effects on the ferromagnetic transition in $Fe_2VAl_{0.95}$, it is expected that resistivity measurement under high pressure provides crucial information. The lattice expansion, $\Delta a/a=0.10\%$ at $\delta=0.05$, can be compensated by applying an experimentally accessible pressure, $\Delta P=3(\Delta a/a)_{\delta=0.05}/\kappa_V\sim 0.5$ GPa, where κ_V is volume compressibility estimated to be 6.81×10^{-3} GPa^{-1} for $\delta=0$.[20] As shown in the inset of Fig. 7,

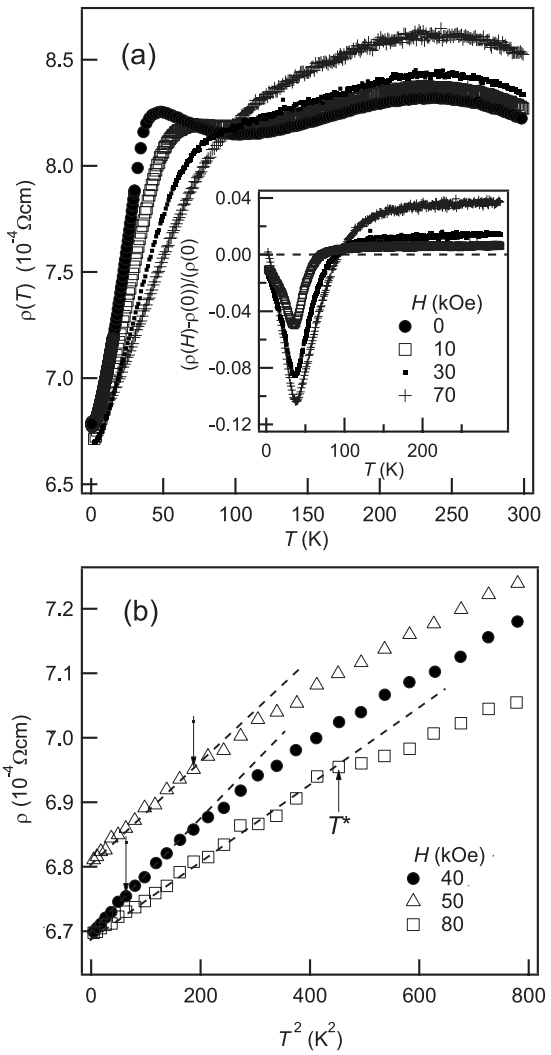

FIG. 6. (a) Resistivity versus temperature of $Fe_2VAl_{0.95}$ in magnetic fields up to 70 kOe as indicated. Inset: Temperature dependence of the magnetoresistance $[\rho(H)-\rho(0)]/\rho(0)$ at $H=10$, 30, and 70 kOe. (b) Resistivity as a function of T^2 at $H=40$, 60, and 80 kOe. The T^2 behavior (dashed lines) is obeyed till a temperature T^* indicated by vertical arrows.

T_{max}^{high} increases while T_{max}^{low} decreases with pressure. The increment of T_{max}^{high} with applying pressure can be responsible for that the pseudo gap locating at the Fermi level increases. On the other hand, the decrement of T_{max}^{low} seems to be related to that of T_C. Pressure dependence of T_C obtained from the temperature variation of $(1/\rho)(d\rho/dT)$ is shown in Figs. 8(a) and 8(b). With increasing pressure the anomalous point shifts toward lower temperature with the pressure coefficient of $(1/T_C)(dT_C/dP)=-0.061$ GPa^{-1} [Fig. 8(b)], which corresponds well with $(1/T_{max}^{low})(dT_{max}^{low}/dP)=-0.074$ GPa^{-1}. The volume effect on T_C is comparable with those for itinerant ferromagnets, such as Ni_3Al [~ -0.10 GPa^{-1} (Refs. 30 and 31)]. Therefore, the emergence of the ferromagnetism at $\delta>0$ can results from mainly the carrier doping in $Fe_2VAl_{1-\delta}$ while the volume expansion seems to be a miner effect. At $T\ll T_C$, it is noteworthy that ρ_0 increases with the pressure coefficient of $(1/\rho_0)(d\rho_0/dP)=0.038$ GPa^{-1} while the exponent of temperature, n, decreases from $n=1.42$ at 0.11 GPa to

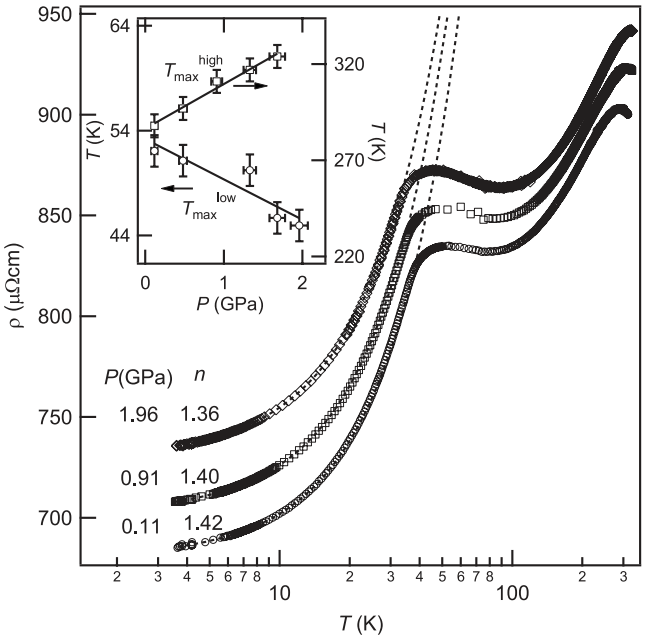

FIG. 7. Resistivity versus temperature of $Fe_2VAl_{0.95}$ at various pressures. Dashed line shows a power low dependence of $\rho(T) \sim AT^n$. The exponent, n, was obtained by fitting $\rho(T)$ to $\rho(T)=\rho_0 + AT^n$ below 11 K. Applied pressure, P, and obtained exponent, n, are indicated on the respective $\rho(T)$ curve. Inset: pressure dependence of the maximum temperatures, T_{max}^{low} and T_{max}^{high}. Solid lines are guides for the eyes.

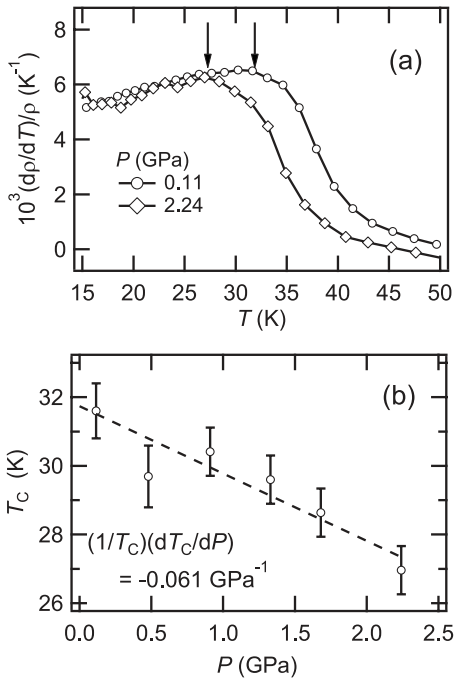

FIG. 8. (a) Temperature dependence of $(1/\rho)(d\rho/dT)$ at various pressures. Arrow indicates Curie point defined as the maximum point of $(1/\rho)(d\rho/dT)$. (b) Pressure variation in T_C. Dashed line represents a fitting curve of T_C versus P obtained by the linear least-squares method.

1.36 at 1.96 GPa, which obtained in a temperature range of $3.5 < T < 11$ K (Fig. 7).

F. Specific heat

In Fig. 9(a) we show the specific heat divided by temperature, C/T, as a function of T^2 measured on $Fe_2VAl_{1-\delta}$ samples with $\delta=-0.05$, 0, and +0.05. A low-temperature upturn as present for $Fe_2VAl_{1.05}$ and Fe_2VAl was also observed previously in Fe_2VAl (Refs. 6 and 8) and in $Fe_{2-x}V_{1+x}Al$.[10] Remarkably, for $Fe_2VAl_{0.95}$ C/T has a strong curvature toward the T^2 axis. Assuming that this curvature in C/T is due to a ferromagnetic spin-wave contribution, $C_{sw} \sim aT^{3/2}$, we fitted the experimental curve at $H=0$ to $C/T=\gamma+a_{sw}T^{1/2}+\beta T^2$ below 20 K [fit not shown in Fig. 9(a)]. The fitting parameters are $\gamma=12.6$ mJ K^{-2} mol^{-1}, $a_{sw}=1.38$ mJ K$^{-5/2}$ mol^{-1}, and $\beta=0.025$ mJ K^{-4} mol^{-1}. However, the presence of the spin-wave contribution in the low-temperature specific heat is not supported by measurements in magnetic field. In field the curvature in C/T enhances significantly. At $H=80$ kOe our fitting procedure results in a larger value for a_{sw}, whereas the spin-wave contribution should be suppressed under magnetic field, as for instance in Ni (Ref. 32) and $CeRu_2Ge_2$.[33] This strongly suggests that the low-temperature variation in $C(T)/T$ is not due to a ferromagnetic spin-wave contribution.

As indicated in Fig. 9(a), the difference in specific heat between $\delta=0$ and -0.05 is quite small except in the low-temperature region where C/T showing an upturn. We fitted the high temperature specific heat, C_{HT}, in the temperature range 8–30 K to $C_{HT}=\gamma T+\beta T^3+\eta T^5$ and estimated $\gamma=3.10\pm0.02$ mJ mol^{-1} K^{-2}, $\beta=0.0265\pm0.0001$ mJ mol^{-1} K^{-4}, and $\eta=(1.82\pm0.02)\times10^{-5}$ mJ mol^{-1} K^{-6} for $\delta=-0.05$, and $\gamma=2.19\pm0.02$ mJ mol^{-1} K^{-2}, $\beta=0.0283\pm0.0001$ mJ mol^{-1} K^{-4}, and $\eta=(1.75\pm0.01)\times10^{-5}$ mJ mol^{-1} K^{-6} for $\delta=0$. These estimated parameters correspond well to those of Fe_2VAl obtained previously in the temperature range 8–25 K.[8]

G. Comparison with paramagnetic Fe_2VAl in the specific heat

Contrasted to the case of $\delta=-0.05$, C/T of $\delta=0.05$ is enhanced obviously compared with that of $\delta=0$. Employing paramagnetic Fe_2VAl as a reference material in the specific heat, the compositional change in $C(T)$, $\Delta C = C(Fe_2VAl_{0.95})-C_{HT}(Fe_2VAl)$ is obtained as shown in Fig. 9(b). Obviously, at zero field a pronounced anomaly is present at $T \approx 34$ K, i.e., at the same temperature where $(1/\rho)(d\rho/dT)$ exhibits a maximum. This anomaly is superposed on the background which has a broad maximum around $T \sim 30$ K [see inset Fig. 9(b)]. The magnetic entropy is obtained by integrating C_{FM}/T versus T and is estimated at 0.7% of R ln 2, where R and C_{FM} are the gas constant and the ferromagnetic component in the specific heat, respectively. Such a small value is expected for a weak itinerant ferromagnet.[19] Below the phase transition point the $\Delta C/T$ curve decreases further with decreasing temperature. Below $T \sim 10$ K the specific heat can be expressed by the sum of linear ($\sim T$) and quadratic ($\sim T^2$) terms. The magnetic field wipes out the magnetic transition anomaly in $\Delta C/T$ and

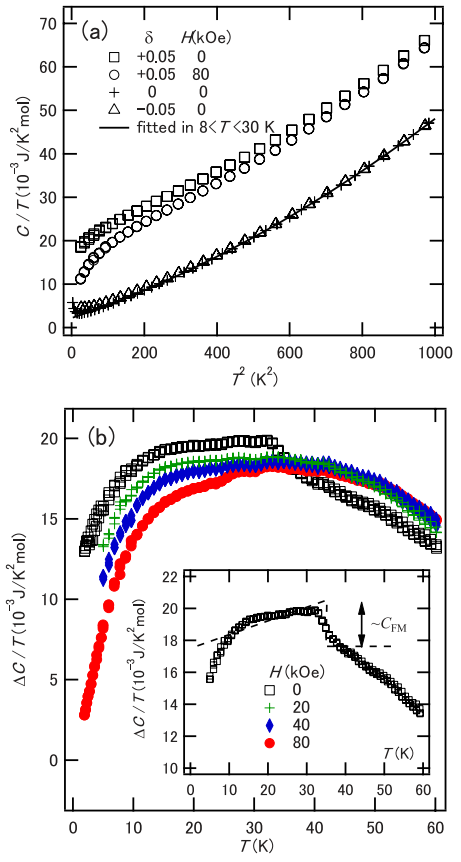

FIG. 9. (Color online) (a) Specific heat divided by temperature C/T plotted as a function of T^2 of $Fe_2VAl_{0.95}$ (δ=+0.05), Fe_2VAl (δ=0), and $Fe_2VAl_{1.05}$ (δ=−0.05) in zero and applied magnetic field. The solid line represents the fit results in the temperature region 8 K$<T<$30 K (see text). (b) Temperature dependence of $\Delta C/T$ defined by $[C(\delta=+0.05)-C(\delta=0)]/T$ at fields of 20, 40, and 80 kOe as indicated. Inset: expanded view of $\Delta C/T$ around the Curie temperature at zero field. The dashed line represents an idealized ferromagnetic contribution, C_{FM}.

causes $\Delta C/T$ to decrease, as shown in Fig. 9(b). An anomalous T^2 temperature dependence in the specific heat was observed also in Pd_2MnIn,[34] GdCu,[35] CuMnSb,[36] and CeNiSn.[37] It seems to be due to a sharp density of state (DOS) shape around E_F, such as the V-shape density of states with small residual component at the Fermi level, as observed in the Kondo insulator CeNiSn.[37] In CeNiSn, at lower temperature the temperature variation in the specific heat shows a deviation from the T-linear dependence, which can be fitted by the sum of a T linear and a T^2 terms.[38] Additionally, the band structure below T_C in $Fe_2VAl_{0.95}$ is more complicated because the ferromagnetic ordering seems to modify considerably the DOS structure due to the exchange splitting, Δ_e, between the spin-up and spin-down bands, which increases effectively with applying external field below T_C. In fact, the low-temperature specific heat $\Delta C \sim \gamma T + \delta T^2$ changes, that is, the ratio of γ/δ decreases upon application of a magnetic field [Fig. 9(b)].

Next, let us discuss quantitatively the comparison between the magnetic moment, μ_p, and carrier concentration, n, modified by the off-stoichiometry in $Fe_2VAl_{0.95}$. As shown in Fig. 6(b), the resistivity follows a quadratic temperature dependence below $T=T^*$, with T^* increasing with magnetic field. The larger value of the coefficient of the T^2 term, $A=10^{-7}-10^{-6}$ Ω cm/K^2, estimated in $Fe_2VAl_{0.95}$ reminds one of the mass enhancement in the stoichiometric samples.[6,8] To compare with the Kadowaki-Woods law, we should consider the small carrier concentration, n, in Fe_2VAl and related alloys.[7,10] In the Fermi-liquid theory, A/γ^2 is proportional to $1/k_F^4$, where γ and k_F are the Sommerfeld constant in the specific heat and the Fermi wave vector, respectively.[39] Compared with heavy fermion systems with $n \approx 1$ (per rare earth or actinide element), it is expected that A/γ^2 is enhanced by a factor of $1/n^{4/3}=2300-360$ in the case of Fe_2VAl since $n=0.003-0.012$.[7] In this estimate, we assumed $k_F \sim n^{1/3}$ given by the Drude model (the free electron model).[40] Therefore, A/γ^2 can be a measure of n, or in other words, the Fermi surface volume. In $Fe_2VAl_{0.95}$, A/γ^2 is 2×10^{-3} Ω cm K^{-2}/(JK^{-2} mol^{-1})^2 being a factor of 40 larger than that established as the Kadowaki-Woods ratio $\sim 1\times10^{-5}$ Ω cm K^{-2}/(JK^{-2} mol^{-1})^2. Therefore, $n \sim 40^{-3/4}=0.063$ per unit formula in $Fe_2VAl_{0.95}$. This value of n is one order of magnitude larger than in Fe_2VAl (Ref. 7) and seems to be consistent with the value of the Hall coefficient of $Fe_2VAl_{0.95}$.[7,12] The observed value $\gamma \approx 12$ mJ mol^{-1} K^{-2} at $H=0$ is rather large when we consider the carrier concentration, $n \approx 0.06$, and the value of normal metals, $\gamma \approx 1$ mJ mol^{-1} K^{-2}. Consequently, the enhancement factor m^*/m_e is $\sim$30, where m_e is the bare electron mass. Compared with the values $\gamma \approx 1.5-2.2$ mJ mol^{-1} K^{-2} and $n=0.003-0.012$ (Ref. 7) in nonmagnetic Fe_2VAl, this large enhancement of γ in ferromagnet $Fe_2VAl_{0.95}$ is surprising because Fe_2VAl is located closer to the magnetic quantum critical point, $T_C \to 0$,[6] where the magnetic fluctuations should be more strongly enhanced. As C/T below T_C has an anomalous temperature and magnetic field dependence, we speculate that the enhancement mechanism of γ distinctly differs from the electron-electron correlation mechanism realized in the heavy fermion systems. Stoichiometric Fe_2VAl is located at the vicinity of a ferromagnetic threshold composition, δ_c. However, not only the Curie temperature, T_C, but also the paramagnetic moment, μ_p, which is strongly dependent on the number of conduction carriers[7,22,23] seem to disappear at $\delta=\delta_c$ in $Fe_2VAl_{1-\delta}$. In contrast, heavy fermion systems show only the magnetic transition temperature, T_M, going to zero while keeping a magnetic moment which has both a localized and an itinerant nature. In other words, the paramagnetic moment does not vanish around the critical point in heavy fermion systems.

IV. SUMMARY

Magnetic, transport, and specific-heat measurements have been carried out on the Heusler-type compound $Fe_2VAl_{0.95}$. The data reveal a ferromagnetic transition takes place at $T_C=33$ K with the characteristics of an itinerant electron ferromagnet. With applying pressure, T_C decreases with the pressure coefficient of $(1/T_C)(dT_C/dP)=-0.061$ GPa^{-1}. The Sommerfeld coefficient in the specific heat is enhanced, $\gamma \approx 12$ mJ mol^{-1} K^{-2}, compared to 3 mJ mol^{-1} K^{-2} in

$Fe_2VAl_{1.05}$ and 2 mJ mol^{-1} K^{-2} in stoichiometric Fe_2VAl. The temperature dependence of resistivity deviates from the characteristics of a Fermi liquid, AT^2, while under magnetic field the quadratic temperature dependence, $\rho(T) \sim T^2$, appears below a certain temperature, T^*, which increases with increasing magnetic field. At lower temperature the temperature variation in the specific heat shows a deviation from the T-linear dependence, especially, under magnetic field, which can be fitted by the sum of a T-linear and a T^2 terms. While the magnetism has a typical characteristics of a weak itinerant ferromagnet, the deviations from the Fermi-liquid characteristics are quite different from those (i.e., non-Fermi-liquid behavior) in a heavy fermion system and a nearly or a weak itinerant ferromagnet.

ACKNOWLEDGMENTS

One of the authors (T.N.) appreciates valuable discussions with Dr. Matsubayashi (ISSP, University Tokyo) and thanks NWO (Dutch Organization for Scientific Research) for a visitor grant.

*Corresponding author. FAX: +81-29-859-2701; naka.takashi@nims.go.jp

[1] R. A. de Groot, F. M. Mueller, P. G. van Engen, and K. H. J. Buschow, Phys. Rev. Lett. **50**, 2024 (1983).
[2] W. E. Pickett and J. S. Moodera, Phys. Today **54**, 39 (2001).
[3] I. Žutić, J. Fabian, and S. D. Sarma, Rev. Mod. Phys. **76**, 323 (2004).
[4] C. Hordequin, D. Ristoiu, L. Ranno, and J. Pierre, Eur. Phys. J. B **16**, 287 (2000).
[5] J. Bœuf, C. Pfleiderer, and A. Faißt, Phys. Rev. B **74**, 024428 (2006).
[6] Y. Nishino, M. Kato, S. Asano, K. Soda, M. Hayasaki, and U. Mizutani, Phys. Rev. Lett. **79**, 1909 (1997).
[7] A. Matsushita, T. Naka, Y. Takano, T. Takeuchi, T. Shishido, and Y. Yamada, Phys. Rev. B **65**, 075204 (2002).
[8] C. S. Lue, J. H. Ross, Jr., C. F. Chang, and H. D. Yang, Phys. Rev. B **60**, R13941 (1999).
[9] H. Matsuda, K. Endo, K. Ooiwa, M. Iijima, Y. Takano, H. Mitamura, T. Goto, M. Tokiyama, and J. Arai, J. Phys. Soc. Jpn. **69**, 1004 (2000).
[10] Y. Nishino, H. Sumi, and U. Mizutani, Phys. Rev. B **71**, 094425 (2005).
[11] T. Nakama, Y. Takaesu, K. Yagasaki, T. Naka, A. Matsushita, K. Fukuda, and Y. Yamada, J. Phys. Soc. Jpn. **74**, 1378 (2005).
[12] Y. Nishino, H. Kato, M. Kato, and U. Mizutani, Phys. Rev. B **63**, 233303 (2001).
[13] Y. Nishino, C. Kumada, and S. Asano, Scr. Mater. **36**, 461 (1997).
[14] T. Naka, T. Adschiri, K. Fukuda, F. Ishikawa, Y. Yamada, Y. Takeuchi, T. Nakama, K. Yagasaki, and A. Matsushita, J. Magn. Magn. Mater. **310**, 1059 (2007).
[15] D. J. Singh and I. I. Mazin, Phys. Rev. B **57**, 14352 (1998).
[16] R. Weht and W. E. Pickett, Phys. Rev. B **58**, 6855 (1998).
[17] G. Y. Guo, G. A. Botton, and Y. Nishino, J. Phys.: Condens. Matter **10**, L119 (1998).
[18] M. Vasundhara, V. Srinivas, and V. V. Rao, Phys. Rev. B **78**, 064401 (2008).
[19] T. Moriya, J. Magn. Magn. Mater. **14**, 1 (1979).
[20] Y. Kawaharada, K. Kurosaki, and S. Yamanaka, J. Alloys Compd. **352**, 48 (2003).
[21] K. Soda, H. Murayama, K. Shimba, S. Yagi, J. Yuhara, T. Takeuchi, U. Mizutani, H. Sumi, M. Kato, H. Kato, Y. Nishino, A. Sekiyama, S. Suga, T. Matsushita, and Y. Saitoh, Phys. Rev. B **71**, 245112 (2005).
[22] F. Ishikawa *et al.* (unpublished).
[23] A. Matsushita *et al.* (unpublished).
[24] N. Môri and T. Mitsui, J. Phys. Soc. Jpn. **26**, 1087 (1969).
[25] R. Saha, V. Srinivas, and T. V. Chandrasekhar Rao, Phys. Rev. B **79**, 174423 (2009).
[26] Y. Takahashi, J. Phys. Soc. Jpn. **55**, 3553 (1986).
[27] K. Ueda, Solid State Commun. **19**, 965 (1976).
[28] J. Takeuchi and Y. Masuda, J. Phys. Soc. Jpn. **46**, 468 (1979).
[29] P. Estrela, A. de Visser, F. R. de Boer, T. Naka, and L. Shlyk, Phys. Rev. B **63**, 212409 (2001).
[30] K. Suzuki and Y. Masuda, J. Phys. Soc. Jpn. **54**, 326 (1985).
[31] N. Buis, J. J. M. Franse, and P. E. Brommer, Physica B & C **106**, 1 (1981).
[32] P. Petrovič, A. Feher, Š. Molokáč, Š. Jánoš, and Košice, Acta Phys. Slov. **31**, 135 (1981).
[33] A. Böhm, R. Caspary, U. Habel, L. Pawlak, A. Zuber, F. Steglich, and A. Loidl, J. Magn. Magn. Mater. **76**, 150 (1988).
[34] G. L. Fraga, D. E. Brandao, and J. G. Sereni, J. Magn. Magn. Mater. **102**, 199 (1991).
[35] N. I. Kourov and Yu. N. Tsiovkin, Sov. J. Low Temp. Phys. **17**, 324 (1991).
[36] S. M. Podgornykh, S. V. Streltsov, V. A. Kazantsev, and E. I. Shreder, J. Magn. Magn. Mater. **311**, 530 (2007).
[37] P. S. Riseborough, Adv. Phys. **49**, 257 (2000).
[38] T. Takabatake, M. Nagasawa, H. Fujii, G. Kido, M. Nohara, S. Nishigori, T. Suzuki, T. Fujita, R. Helfrich, U. Ahlheim, K. Fraas, C. Geibel, and F. Steglich, Phys. Rev. B **45**, 5740 (1992).
[39] K. Yamada, *Electron Correlation in Metals* (Cambridge University Press, Cambridge, 2004), Chap. 7, p. 141.
[40] N. W. Ashcroft and N. D. Mermin, *Solid State Physics* (Saunders, Philadelphia, 1976), Chap. 2, p. 36.